AAPS PharmSciTech, Vol. 11, No. 3, September 2010 (© 2010)
DOI: 10.1208/s12249-010-9496-7

Research Article

Formulation of Dacarbazine-loaded Cubosomes. Part III. Physicochemical Characterization

Di Bei,[1] Tao Zhang,[1] James B. Murowchick,[2] and Bi-Botti C. Youan[1,3]

Received 16 March 2010; accepted 23 July 2010; published online 6 August 2010

Abstract. The purpose of this study was to investigate the physicochemical properties of dacarbazine-loaded cubosomes. The drug-loaded cubosome nanocarriers were prepared by a fragmentation method and then freeze dried. They were then characterized for size, morphology, thermal behavior, and crystallography using dynamic light scattering, transmission electron microscopy (TEM), differential scanning calorimetry (DSC), and powder X-ray diffraction (PXRD), respectively. The drug loading and encapsulation efficiency were determined by UV spectrophotometry. The results showed that the prepared dacarbazine-loaded cubosomes had mean diameters ranging from 86 to 106 nm. In addition to the TEM, the characteristic peaks from PXRD data suggested that the freeze-dried nanoformulations were indeed cubic in nature. DSC and PXRD analysis suggested the 0.06 or 0.28% *w/w* actual drug loaded inside cubosomes was in the amorphous or molecular state. These physicochemical characteristics would affect the nanoformulation shelf-life, efficacy, and safety.

KEY WORDS: cubosome; dacarbazine; thermal analysis; X-ray diffraction.

INTRODUCTION

In several recent studies, powder X-ray diffraction (PXRD), and differential scanning calorimetry (DSC) have been proven to be useful tools in drug formulation characterization. These include indinavir-loaded microparticle (1,2) controlled-release baclofen tablets (3) bacterial cellulose (4), and solid state amoxicillin trihydrate (5). These drug formulation characterization approaches have been recently used for nanosuspension formulation as well (6). Dacarbazine (DTIC, Fig. 1a), a water-soluble drug, is currently used as a first-line chemotherapy medication against melanoma (7,8). However, current delivery methods are not ideal. For example, this reference drug in melanoma therapy is potent (9), but it has some serious side effects. It is normally administered intravenously, which is painful and reduces patient compliance. Secondly, the absorption of dacarbazine is generally erratic, slow, and incomplete. For example, even after intravenous administration at a starting dose of 250 mg/m^2 in a study conducted with 17 subjects indicated, the time of occurrence of peak concentration, maximum concentration, and area under the curve were 0.5 h (CV=25%), 10.2 μg/mL (CV=44%), and 16 μg/h/mL (CV=69%), respectively. Here, CV indicated the coefficient of variation (10). Thirdly, the drug is light sensitive and unstable. Fourthly, DTIC is myelosuppressive, and its use in combination therapy has been further limited by its short half-life (11). One promising strategy to overcome these limitations is to encapsulate this drug using nanocarriers or nanoparticulate systems intended for controlled drug delivery.

Cubic phase gels are gaining interest in drug delivery (12). In analogy with the liposomal dispersions, nonlamellar phase particles can be prepared by dispersion formation in a multiphase region comprising a liquid crystal in coexistence with a dilute aqueous phase. Such particles were first observed in a study of fat digestion (13). The cubic phase of hydrated monoolein was reported to serve as an appropriate environment in which to grow crystals of some membrane proteins (14,15). Cubosomes are fundamentally different from the solid lipid nanoparticles described by Muller *et al.* (16) in term of their nanostructure, chemical composition, and production method.

In recent studies, this research group proposed cubosomes (cubosome dispersions) as alternative nanocarrier for this drug (15,16). However to our knowledge, the physicochemical properties of this specific nanoformulation are not yet fully elucidated. The present study was concerned with the first characterization of dacarbazine-loaded cubosomes using techniques such as dynamic light scattering, electron microscopies, DSC, and PXRD to provide further insight on their size, morphology, thermal behavior, and crystalline properties. The central goal of this study was specifically to shed light into the nano-structure of DTIC-loaded cubosomes.

[1] Laboratory of Future Nanomedicines and Theoretical Chronopharmaceutics, Division of Pharmaceutical Sciences, University of Missouri-Kansas City School of Pharmacy, 2464 Charlotte, Kansas City, Missouri 64108, USA.
[2] Department of Geosciences, University of Missouri, 420 Flarsheim Hall, 5110 Rockhill Rd, Kansas City, Missouri 64110, USA.
[3] To whom correspondence should be addressed. (e-mail: youanb@umkc.edu)

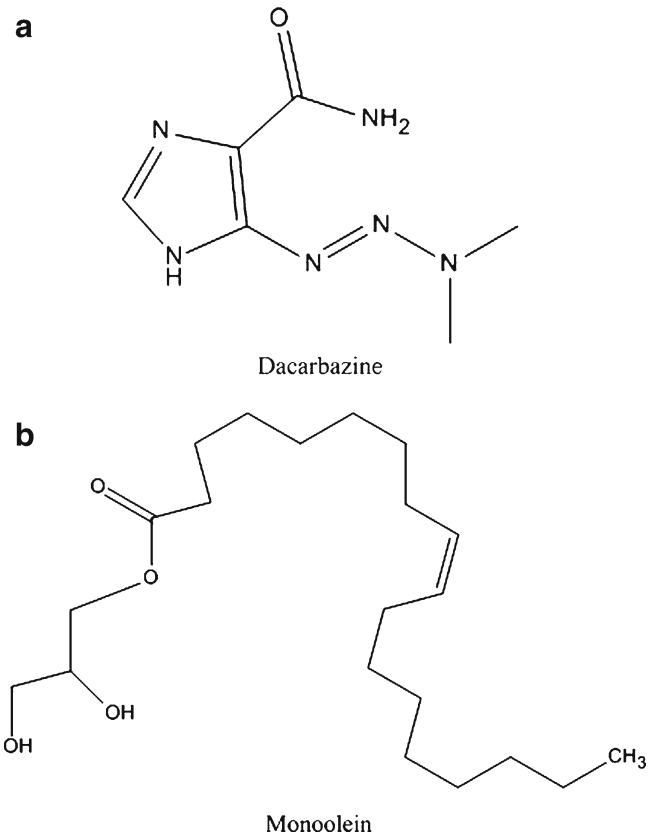

Fig. 1. Selected physicochemical properties of key ingredients used in the cubosome nanoformulation: **a** Dacarbazine, (DTIC, $C_6H_{10}N_6O$, pka: 4.42, MW: 182.18, mp: ~205°C, water solubility: 4220 mg/L, logP= −1.6; 38); **b** Monoolein (GMO, $C_{21}H_{30}O_4$)

MATERIALS AND METHODS

The glycerol monooleate RYLO MG 19 (GMO, Fig. 1b) was kindly donated by Danisco Cultor (Grindsted, Denmark). Poloxamer 407 (F127, MW=9,840–14,600) was kindly donated by BASF Corporation (Ludwigshafen, Germany). Phosphate buffer saline (PBS) and DTIC (5-(3, 3-Dimethyl-1-triazeno) imidazole-4-carboxamide) were purchased from Sigma Aldrich (St. Louis, MO, USA). Chloroform was purchased from Fisher Scientific (Pittsburgh, PA, USA). All chemicals used in the study were of analytical grade and used without further purification.

Preparation of Dacarbazine-loaded Cubosomes

The method of preparation of DTIC-loaded cubosomes was adapted from previous work of Esposito *et al.* (17–19). Briefly, for each sample, a volume of 15 ml chloroform was used to completely dissolve 500 mg GMO and 75 mg F127. The flask was then attached to a rotavapor (WK 300 Lauda, Buchi Laboratoriums-Technik AG, Flawil, Switzerland) to evaporate chloroform at 60 rpm, and at the temperature of 60°C±2°C for 15 min. After evaporation, which was confirmed using mass balance to verify that the cold trap was actually capturing all the chloroform, a thin film was formed at the bottom of the flask. A volume of 50 ml of PBS buffer saline (pH=7.4) was used to dissolve the drug and this solution was added into the dry lipid film to form coarse dispersions. A sonicator (MODEL 150D, VWR Inc., West Chester, PA, USA) was used to briefly mix the lipid film and water phase together. This coarse dispersion was maintained at the desired temperature of 76 or 80°C±2°C (depending on the sample to be prepared) for 15 min in a water bath (BS-06 Lab. Companion, Jeio Tech Co., LTD, Seoul, Korea). The hot mixture was swiftly transferred to a beaker in which a homogenizer (IKA ULTRA-TURRAX T-25, Staufen, Germany) was used to prepare uniform dispersion. Cubosomes were formed as the dispersion gradually cooled down to room temperature. Aluminum coils were used to cover the sample vials in order to protect samples from direct light. The dispersions were then ready for future tests and evaluation.

Encapsulation Efficiency

The encapsulation efficiency (Y_2) was measured at the wavelength of 330 nm with a UV spectrometer (NanoDrop Model 1000, Thermo Fisher Scientific, DE, USA). This spectrometer enables highly accurate UV/Vis analyses of 1 μl samples with remarkable reproducibility. The standard curve, based on the DTIC concentration from 0 to 360 μg/ml, had a regression equation of $y=0.0061x-0.0081$ with R^2 of 0.9985. In this study, all UV measurements and calculations of Y_2 were based on this specific equipment and standard curve. In all experimental trials, the measurement of the encapsulation efficiency (EE) was carried out with one specific kind of centrifuge tube, Amicon Ultra 3,000 MWCO (Millipore, Billerica, MA, USA). Preliminary studies conducted with known concentrations of drug from the calibration curve showed that this specific drug did not significantly bind to the membrane Ultra 3,000. Moreover, the UV molar absorptivity (ε~11,200 L/molcm) did not change significantly for the free and encapsulated drug forms. In each experiment, the room temperature sample was transferred to tubes and centrifuged at 1,500 rpm for 30 min. The non-encapsulated drug or free drug form in solution leaked outside the sub-tubes, making it possible to measure each concentration in solution, and thus allowed the estimation of the amount of drug encapsulated into cubosomes. The UV absorbance at total concentration was labeled as C_t and the UV absorbance of DTIC contained in filtrate after centrifuge was labeled as C_f (namely, filtrate concentration). Thus, the encapsulation efficiency was calculated as follows:

$$EE\% = \left[\left(C_t - C_f\right) \div C_t\right] \times 100 \quad (1)$$

Particle Size Determination

The particle size of the cubosomes was determined through dynamic light scattering (DLS, Brookhaven Instruments Corporation, Austin, TX, USA). DLS, sometimes referred to as photon correlation spectroscopy, which is a non-invasive, well-established technique for measuring the size of molecules and particles typically in the submicron region. The measurements were taken at a temperature of 25°C, a laser wavelength of 659.0 nm, and a refractive index of 1.330. The samples were vortexed before measuring the particle size. In this study, particle size and size distribution

(polydispersity, PI) of cubosome samples were measured. The samples were vortexed before measuring the particle mean diameter (z average), size distribution, and polydispersity of the cubosomes. Based on National Institute standard, a sample with a PI<0.05 was considered monodispersed (20).

Transmission Electron Microscopy

The samples were prepared by putting a 5-μl droplet of the cubosome suspension onto a 300-mesh carbon-coated copper grid, and letting the cubosomes settle for 3–5 min. Then, the excess fluid was removed by wicking it off with an absorbent paper. Samples were negatively stained in 1% uranyl acetate for 3–5 min. The samples were then viewed on a JEOL Model JEM 1400 120KV transmission electron microscope (JEOL-USA, Wilmington, DE, USA) and photographed digitally on a Gatan axis-mount 2k×2k digital camera.

Powder X-Ray Diffraction (PXRD) Measurement

PXRD slow scan image of drug-containing cubosomes, pure dacarbazine crystal was used under X-ray measurement. In addition, four selected samples were also chosen and are hereafter referred to as sample F1+, F1−, F2+, F2−. These samples were the optimized formulation based on formulation variable studies (18) (numbered 2, or F1+) and its drug-free control (numbered 1 or F1−), the optimized formulation from process parameters study (numbered 4 or F2+), and its drug-free control (numbered 3 or F2−). In the rotating crystal method, a single crystal was mounted with an axis normal to a monochromatic X-ray beam. A cylindrical film was placed around it and the crystal was rotated about the chosen axis. As the crystal rotated, a set of lattice planes at some point made the correct Bragg angle for the monochromatic incident beam resulting in the formation of a diffracted beam. The reflected beams were located on the surface of imaginary cones. When the film was laid out flat, the diffraction spots laid on horizontal lines. Samples were freeze dried prior to testing. The temperature differences were controlled within 0.1°C. Filtered radiation and a graphite monochrometer were employed. The diffraction angle covered from 2θ=20–90°. The inner equipment along with the solid sample was put under vacuum to minimize air scattering. Diffraction patterns were monitored and recorded by the detector. They were compared to crystallographic database using software database (Jade version 8.0, Materials Data Inc., Livermore, CA, USA).

Differential Scanning Calorimetry (DSC) Analysis

DSC experiments were performed on a Perkin Elmer DSC 7 (Waltham, MA, USA) to determine the physical state of the drug-encapsulated separate. Five selected samples were chosen: the two formulations F1+, F2+ described above and three other samples composed of native GMO, native F127 samples, and native DTIC sample. Approximately 1–2 mg of each freeze-dried sample was sealed in aluminum pans. The DSC scans were performed from 25–450°C at a heating rate of 10°C/min in a nitrogen atmosphere. The crystallinity of the sample was examined by studying the location and width of the melting peak.

RESULTS AND DISCUSSION

Dacarbazine-loaded Cubosome Morphology and Drug Loading

Sample #1 and control #1 were formulated using the authors' published method related to the study of formulation variables (18). Basically, drug-loaded sample #1 (F1+) and control #1 (blank cubosomes, F1−) were prepared in the same condition, namely at homogenization speed of 13,500 rpm for 1 min duration at 80°C±2°C. These process parameters were selected based on reliable and detailed temperature-composition phase diagrams of monoolein/water system available in the literature (21,22). The literature concerning monoolein/water miscibility suggests a three-stage development in our understanding of the system. In the 1965 work of Lutton (23), the first stage was described based on consistency and polarized light microscopy leading to the identification of the major phases (Lα, cubic, inverted hexagonal). In the second stage, X-ray diffraction and NMR-based diffusion measurements were performed (24). It was in this period that the different cubic phases were identified. The third stage shed more light on the miscibility properties and attempts to characterize the true equilibrium behavior of the system by various procedures (21,25). However, most of these basic physical chemistry studies did not involve a drug such as dacarbazine, thus indicating the need for further study.

The first preparation conditions (using 100 mg of GMO, 107 mg of F 127 and 2 mg of DTIC as independent variables) led to the production of drug loaded cubosomes with 106.1± 0.8 nm (n=3) in mean diameter and 6.9% in EE%. The actual drug loading in F1+ was 0.06% *w*/*w*. The particle size for sample F1− was similar to that of F1+. The relatively low EE% may be due to the rapid diffusion of the drug in the aqueous phase during the preparation and the centrifugation processes. Previous studies reported that even lipophilic drugs were rapidly released from cubosomes after ultrafiltration (26). However, sample #2 (F2+) and control #2 (F2−) were prepared using the method resulting from the process parameters study (19). In this case, using 500 mg of GMO, 75 mg of F127, and 10 mg of DTIC, minimal particle size was achieved with approximately 24,000 rpm of homogenization speed, 5.4 min of duration, at 76°C±2°C temperature. These process parameters resulted in the production of drug-loaded cubosomes of 88.4±1.3 nm (n=3) in size and 16.7% in EE%. The actual drug loading in F2+ was 0.28 *w*/*w*. This represented approximately fourfold more drug loading compared to that of sample F1+. This difference in EE% may be explained by the use of approximately 2.8-fold more cubosome matrix-forming materials (GMO+F127) and fivefold more drug used at the beginning of this second formulation process. In this case, the sizes of the sample F2+ and F2− were in the same range as well. However, the significant size difference between sample F1+ and F2+ may be explained by the difference in the speed of homogenization, as a significantly higher speed was used in the F2+ and F2− production. Typical electron micrograph is shown in Fig. 2 indicating that cubosomes were indeed formed. Figure 2a shows a population of drug loaded cubosomes observed at low magnification while Fig. 2b shows a single cubosome at relatively high magnification. These observations were further confirmed by X-ray diffraction and DSC analysis as discussed in the section below.

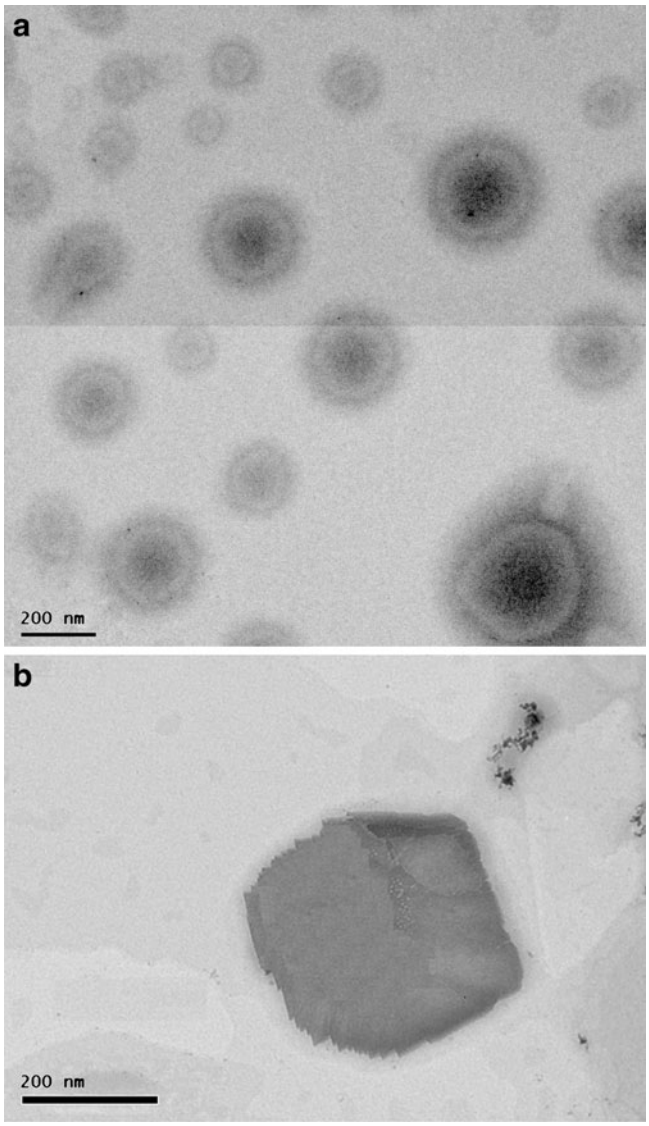

Fig. 2. Typical TEM image of dacarbazine loaded cubosome nanocarrier: **a** a population of cubosomes. **b** Single cubsome to better view the cubic structure. *Scale bar* 200 nm

Powder X-Ray Diffraction Measurement

X-ray diffraction measurement was used to understand the inner structure of the cubosomes and it served as additional evidence of cubic structure formation. Figure 3 shows the PXRD of native DTIC exhibiting a characteristic peak at 38°. From published three-dimensional X-ray data, the crystal structure of this drug has been reported (27) as monoclinic with space group $P2_1/n$, with a=14.042 (2), b=10.661 (2), c=11.914 (4) Å, β=91.49 (8), V=1783.0 (8) Å3, Z=8. The asymmetric unit contains two molecules. In one molecule, the protonated N in the imidazole ring is adjacent to the triazene group, and in the other, it is adjacent to the carboxamide group. Each molecule is approximately planar and contains an internal N-H…N hydrogen bond. Intermolecular hydrogen bonding produces sheets of molecules lying approximately perpendicular to the *b*-axis (27). Macroscopically, DTIC also occurs as white to ivory-colored microcrystals that are soluble in water.

Figure 4 shows the PXRD of the two DTIC-loaded cubosome samples (F1+, F2+) and their respective controls (F1−, F2−). In this Fig. 4, the *x*-axis represents the scattering angle (denoted as 2θ) and *y*-axis the light's intensity. For all four samples, two characteristic peaks were visible at around 44° and 52°, respectively. These two peaks represented the aluminum holder's peaks. The peaks that are located at around 36°, 54°, and 66°, respectively, were found to be characteristic of the cubic crystals. This observation was consistent with previously reported ones using other advanced techniques (17,28,29). It has been shown that the PXRD spectrum of pure F127 nanospheres exhibited two characteristic peaks representing a high degree of ring-like crystallization of the F127 (30). However, these peaks were not detectable in the analyzed samples, probably due to the dramatic F127 diffusion in the aqueous phase during the preparation process. This process significantly reduced the residual amount of F 127 in the final cubosome.

Landh (31) studied the phase diagram of the ternary GMO/water/F127 system in depth. He found that the cubic phase extends through a wide range of water (up to 67 wt.%) and a maximum polymer content of 20 wt.%. Larsson also reproduced the obtained partial phase diagram in a simplified manner (28). These studies showed that F127 is incorporated into the monophasic GMO-based cubic phase region, which induces transitions between different cubic symmetries and significantly enhances the water solubilization capacity of these self-assembled systems. Unfortunately, the limitation in detection of the PXRD instrument used in this study did not allow these observations.

It has also been shown that GMO forms in excess water saddle-like curved bilayers (bicontinuous cubic Pn3m-phase with negative membrane curvature) (22). A simple approach to explain the principle governing the cubosome formation process was given by the critical packing parameter γ as shown in Eqs. 2 and 3 below (22).

$$\gamma = \frac{V}{A(l)l} \tag{2}$$

$$\gamma = \frac{\phi_l a^3}{2l(A_0 a^2 + 2\pi\chi l^2)} \tag{3}$$

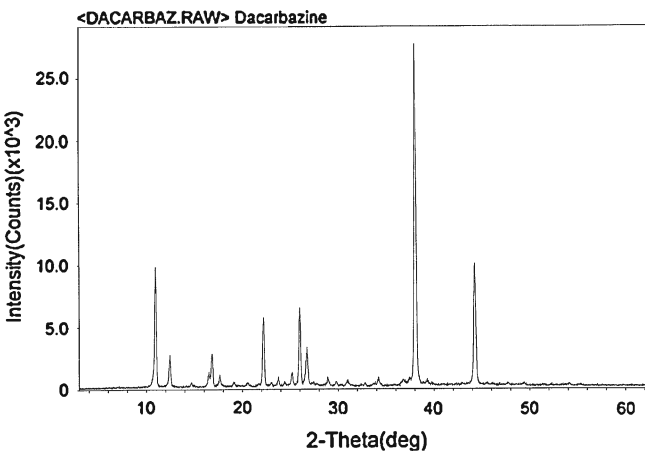

Fig. 3. PXRD pattern of native DTIC

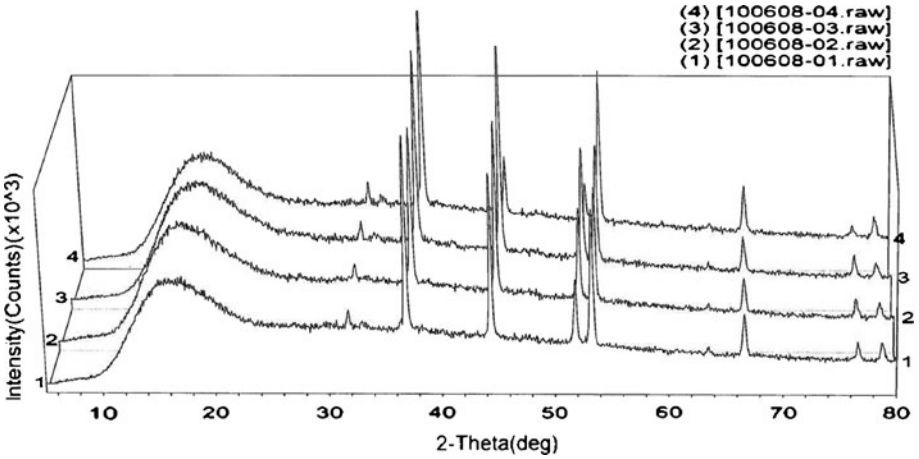

Fig. 4. PXRD pattern of four samples: first drug-free or blank cubosome (number 1, sample F1−) and corresponding master cubsome formulation based on formulation variable (number 2, sample F1+), second blank cubosome (number 3, sample F2−) and corresponding master formulation based on process parameters (number 4, sample F2+)

where V is the lipid molecular or hydrophobic chain volume, $A(l)$ is the lipid head group area, l is the lipid or hydrophobic chain length, ϕ_l is the volume fraction of lipid in the unit cell (estimated as the weight fraction of lipid in the sample based on the assumption that lipid and water density are equal; (32). a is the cubic phase lattice parameter, and A_0 and χ are the ratio of the minimal surface in the unit cell to the quantity (unit cell volume)$^{1/3}$ and the Euler–Poincare characteristic, respectively. In the case of the Pn3m phase, A_0=1.919 and χ=−2 (33). For GMO, γ>1 (22) and this value is temperature dependent. One consequence of a larger γ is that the lipid/water interface is more highly curved and the phase can accommodate less water. This could also explain the poor loading of a water-soluble drug such as DTIC into these cubosomes.

Collectively, the PXRD data confirmed the existence of the cubic structure. However, in Fig. 4, any characteristic peak pointing towards DTIC's crystal existence was not apparent suggesting that the drug was encapsulated in cubosomes in an amorphous or molecular state. However, as the crystal detection level of the equipment used was limited, the small amount of DTIC may have been shielded and thus could not be detected. To confirm this speculation, DSC analysis was further performed as described below to further evaluate if the drug was indeed encapsulated inside the cubosomes in crystalline form or amorphous form.

Overall, the X-ray diffraction results were in agreement with the transmission electron microscopy (TEM) observations (Fig. 2), revealing the existence of a cubic organization. It should be emphasized that it is not possible by this TEM and PXRD method to unambiguously determine the exact nature of these nanostructures formed. Based on published data in similar systems, the authors reasonably speculated the coexistence of two different cubic phases, the first being a bicontinuous cubic phase of spatial symmetry Im3m (Q^{229}) and the second belonging to the Pn3m (Q^{224}) spatial symmetry (17,34,35). The intensity of the Pn3m peaks may be quite lower with respect to the intensities related to the Im3m phase. It has also been reported that the internal structural transition from Pn3m to Im3m depends on the polymeric stabilizer's concentration (36). However, the transition of Lα to Im3m as a result of the membrane fusion processes (37) takes place through the interplay of the following steps: (1) enhancement of the lipid chain fluidity, (2) water uptake, and (3) penetration of F127 into the membrane surfaces. Future studies involving cryo-TEM and small angle X-ray scattering are needed to further elucidate these specific drug-loaded cubic structures.

Thermal Analysis

In this study, DSC was used to evaluate the physical status of the drug within the cubosomes. The results are shown in Fig. 5. Figure 5a–c represented native monoolein, polymer (F 127) and DTIC, respectively. Figure 5d–e represented optimized formulation F1+ and F2+, respectively. In addition to the drug's thermogram, all samples analyzed exhibited a melting endotherm followed by degradation peaks at higher temperatures. Specifically, in native GMO thermogram (Fig. 5a), the melting temperature peak was around 37°C and consistent with the manufacturer product data sheet.

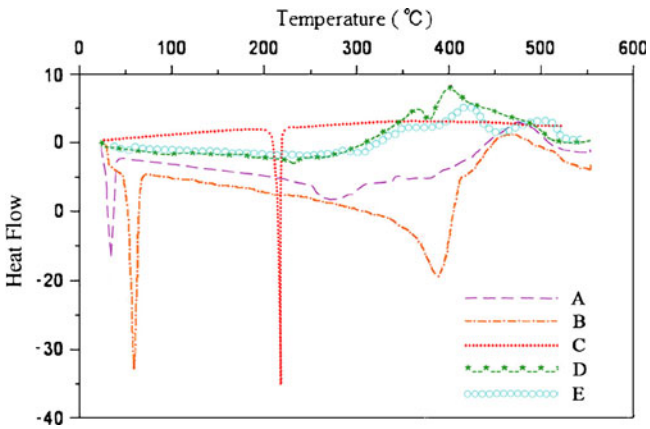

Fig. 5. DSC Thermograms of **a** native monoolein (GMO), **b** native poloxamer 407 (F 127), **c** native dacarbazine (DTIC), **d** cubosome formulation based on formulation variables (F1+), and **e** cubosome formulation based on process parameters (F2+). *Downwards direction* endothermic, *upwards direction* exothermic

Moreover, this thermal behavior was similar to that observed while heating GMO and tricaprylin. Moreover, decreasing the GMO fraction led to a decrease in the enthalpy of the endothermic peak observed around its current melting point from 20 (pure GMO) to 6 J g^{-1} (GMO/tricaprylin 75/25), indicating that increasing quantities of GMO were dissolved in the tricaprylin (38). These observations may explain the dramatic decrease of the enthalpy of fusion of GMO when mixed with drugs and the polymer (Fig. 5d–e).

In a native F 127 thermogram (Fig. 5b), the endothermic peak was around 56°C and was also consistent with the manufacturer product data sheet.

In the native DTIC thermogram (Fig. 5c), the melting temperature peak was sharp, around 200°C. This peak was also consistent with other literature data. In thermogram D and E, the melting peaks of GMO and F 127 were not well distinguishable perhaps due to the plasticizing effect of GMO within the polymer chains. Both ingredients of the cubosomes seem to melt together in temperatures ranging from around 37°C to around 56°C which may be the result of the plasticizing effect of GMO. The thermal events around those related to the drug's melting point were different from those of the native drug (no sharp drug melting peak at around 200°C). The thermal events observed between 200°C and 300°C may be related to GMO degradation process, as observed in Fig. 5a. Therefore, consistent with the above PXRD data, it was concluded that DTIC encapsulated in cubosomes were not in crystal form in the two cubosome nanoformulations.

CONCLUSION

Taken together, PXRD and DSC analyses suggest that the formulated dacarbazine-loaded cubosomes exhibited a cubic crystalline structure. The drug (dacarbazine) that was encapsulated in a loading range of 0.06–0.28 *w*/*w* inside the cubosomes was in the amorphous or molecular state in these nanoformulations. These physicochemical characteristics which determine drug crystallization kinetics during storage, its chemical reactivity and mechanical properties would affect the nanoformulation shelf-life, efficacy, and safety (37). In this preclinical and preliminary study, a mass balance was used to estimate the complete solvent removal. However, organic solvents are difficult to remove quantitatively and thus some traces usually remains in such particulate systems (39,40). The potential impact of the residual solvent on drug loading within cubosomes, the nanosystem stability and cubosomes' properties remains to be elucidated. Moreover, considering the International Conference on Harmonisation requirements of a very low limit of 60 ppm for chloroform in pharmaceuticals intended for human use (41), alternative methods would be required to minimize the organic solvent levels in these nanosystems. These might include drying at relatively higher temperatures and reduced pressure (42), extraction using super critical carbon dioxide (39) or radiolysis (43) followed by gas chromatography mass spectroscopy analysis. Further experiments should also use alternative crystallographic and imaging techniques to further elucidate these nanostructures. Moreover, to enhance drug loading and efficacy, *in vitro* release profile, compatibility and stability studies, and *in vivo* studies will be needed to fully exploit the potential of cubosomes in melanoma or other diseases' treatment.

ACKNOWLEDGMENTS

Monoolein (GMO) was kindly provided to us by Danisco Cultor (Grindsted, Denmark). We also appreciated the guidance of Dr. Elizabeth Kostoryz (Division of Pharmacology, University of Missouri–Kansas City) for the DLS experiment and the support of Randy Tindall (Electron Microscopy Center, University of Missouri–Columbia) for the electron microscopy. The author acknowledge the helpful and thorough proof reading of this manuscript by Margaret LoGiudice, R.D.H, M.S. (Johnson County Community College, Overland Park, KS)

REFERENCES

1. Chiappetta DA, Carcaboso AM, Bregni C, Rubio M, Bramuglia G, Sosnik A. Indinavir-loaded pH-sensitive microparticles for taste masking: toward extemporaneous pediatric anti-HIV/AIDS liquid formulations with improved patient compliance. AAPS PharmSciTech. 2009;10(1):1–6.
2. Hancock BC, Zografi G. Characteristics and significance of the amorphous state in pharmaceutical systems. J Pharm Sci. 1997;86 (1):1–12.
3. Abdelkader H, Abdalla OY, Salem H. Formulation of controlled-release baclofen matrix tablets: influence of some hydrophilic polymers on the release rate and *in vitro* evaluation. AAPS PharmSciTech. 2007;8(4):E100.
4. Kaewnopparat S, Sansernluk K, Faroongsarng D. Behavior of freezable bound water in the bacterial cellulose produced by *Acetobacter xylinum*: an approach using thermoporosimetry. AAPS PharmSciTech. 2008;9(2):701–7.
5. Ghassempour A, Rafati H, Adlnasab L, Bashour Y, Ebrahimzadeh H, Erfan M. Investigation of the solid state properties of amoxicillin trihydrate and the effect of powder pH. AAPS PharmSciTech. 2007;8(4):E93.
6. Van Eerdenbrugh B, Stuyven B, Froyen L, Van Humbeeck J, Martens JA, Augustijns P, *et al*. Downscaling drug nanosuspension production: processing aspects and physicochemical characterization. AAPS PharmSciTech. 2009;10(1):44–53.
7. Spieth K, Kaufmann R, Dummer R, Garbe C, Becker JC, Hauschild A, *et al*. Temozolomide plus pegylated interferon alfa-2b as first-line treatment for stage IV melanoma: a multicenter phase II trial of the Dermatologic Cooperative Oncology Group (DeCOG). Ann Oncol. 2008;19(4):801–6.
8. Schadendorf D, Ugurel S, Schuler-Thurner B, Nestle FO, Enk A, Brocker EB, *et al*. Dacarbazine (DTIC) *versus* vaccination with autologous peptide-pulsed dendritic cells (DC) in first-line treatment of patients with metastatic melanoma: a randomized phase III trial of the DC study group of the DeCOG. Ann Oncol. 2006;17(4):563–70.
9. Lens MB, Eisen TG. Systemic chemotherapy in the treatment of malignant melanoma. Expert Opin Pharmacother. 2003;4 (12):2205–11.
10. Middleton MR, Grob JJ, Aaronson N, Fierlbeck G, Tilgen W, Seiter S, *et al*. Randomized phase III study of temozolomide *versus* dacarbazine in the treatment of patients with advanced metastatic malignant melanoma. J Clin Oncol. 2000;18(1):158–66.
11. Connors TA, Goddard PM, Merai K, Ross WC, Wilman DE. Tumour inhibitory triazenes: structural requirements for an active metabolite. Biochem Pharmacol. 1976;25(3):241–6.
12. Shah JC, Sadhale Y, Chilukuri DM. Cubic phase gels as drug delivery systems. Adv Drug Deliv Rev. 2001;47(2–3):229–50.
13. Patton JS, Carey MC. Watching fat digestion. Science (New York, NY). 1979;204(4389):145–8.
14. Pebay-Peyroula E, Rummel G, Rosenbusch JP, Landau EM. X-ray structure of bacteriorhodopsin at 2.5 angstroms from microcrystals grown in lipidic cubic phases. Science (New York, NY). 1997;277 (5332):1676–81.

15. Landau EM, Rosenbusch JP. Lipidic cubic phases: a novel concept for the crystallization of membrane proteins. Proc Natl Acad Sci USA. 1996;93(25):14532–5.
16. Muller RH, Petersen RD, Hommoss A, Pardeike J. Nanostructured lipid carriers (NLC) in cosmetic dermal products. Adv Drug Deliv Rev. 2007;59(6):522–30.
17. Esposito E, Eblovi N, Rasi S, Drechsler M, Di Gregorio GM, Menegatti E, *et al*. Lipid-based supramolecular systems for topical application: a preformulatory study. AAPS PharmSci. 2003;5(4):E30.
18. Bei D, Marszalek J, Youan BB. Formulation of dacarbazine-loaded cubosomes-part I: influence of formulation variables. AAPS PharmSciTech. 2009;10(3):1032–9.
19. Bei D, Marszalek J, Youan BB. Formulation of dacarbazine-loaded cubosomes—part II: influence of process parameters. AAPS PharmSciTech. 2009;10(3):1040–7.
20. Hackley VaF CF. The use of nomenclature in dispersion science and technology, NIST recommended practice guide. SP. 2001;960 (3):76.
21. Briggs J, Chung H, Caffrey M. The temperature composition phase diagram and mesophase structure characterization of the monoolein/water system. J Phys II France. 1996;6:723–51.
22. Qiu H, Caffrey M. The phase diagram of the monoolein/water system: metastability and equilibrium aspects. Biomaterials. 2000;21(3):223–34.
23. Lutton ES. Phase behavior of aqueous systems of monoglycerides. J Am Oil Chem Soc. 1965;42(12):1068–70.
24. Longley W, McIntosh TJ. A bicontinuous tetrahedral structure in a liquid-crystalline lipid. Nature. 1983;303:612–4.
25. Hyde ST, Anderson S, Ericsson B, Larsson K. A cubic structure consisting of a lipid bilayer forming an infinite periodic minimum surface of the gyroid type in the glyceryl monooleate-water system. Z Kristallogr. 1984;168:213–9.
26. Boyd BJ. Characterisation of drug release from cubosomes using the pressure ultrafiltration method. Int J Pharm. 2003;260(2):239–47.
27. Freeman HC, Hutchinson ND. The crystal structure of the anti-tumor agent 5-(3, 3-dimethyl-1-triazenyl)imidazole-4-carboxamide (NSC-45388). Acta Cryst B. 1979;35:2051.
28. Yaghmur A, Laggner P, Almgren M, Rappolt M. Self-assembly in monoelaidin aqueous dispersions: direct vesicles to cubosomes transition. PLoS ONE. 2008;3(11):e3747.
29. Esposito E, Cortesi R, Drechsler M, Paccamiccio L, Mariani P, Contado C, *et al*. Cubosome dispersions as delivery systems for percutaneous administration of indomethacin. Pharm Res. 2005;22 (12):2163–73.
30. Liu TY, Hu SH, Liu KH, Shaiu RS, Liu DM, Chen SY. Instantaneous drug delivery of magnetic/thermally sensitive nanospheres by a high-frequency magnetic field. Langmuir. 2008;24(23):13306–11.
31. Landh T. Phase behavior in the system pine oil monoglycerides-poloxamer 407-water at 20 C. J Phys Chem. 1994;98:8453–67.
32. Israelachvili JN. Intermolecular and surface forces. London, UK: Academic; 1991.
33. Anderson DM, Gruner SM, Leibler S. Geometrical aspects of the frustration in the cubic phases of lyotropic liquid crystals. Proc Natl Acad Sci USA. 1988;85(15):5364–8.
34. Siekmann B, Bunjes H, Koch MH, Westesen K. Preparation and structural investigations of colloidal dispersions prepared from cubic monoglyceride-water phases. Int J Pharm. 2002;244 (1–2):33–43.
35. Worle G, Drechsler M, Koch MH, Siekmann B, Westesen K, Bunjes H. Influence of composition and preparation parameters on the properties of aqueous monoolein dispersions. Int J Pharm. 2007;329(1–2):150–7.
36. Gustafsson J, Ljusberg-Wahren H, Almgren M, Larsson K. Submicron particles of reversed lipid phases in water stabilized by a nonionic amphiphilic polymer. Langmuir. 1997;13:6964–71.
37. Hui SW, Stewart TP, Boni LT, Yeagle PL. Membrane fusion through point defects in bilayers. Science (New York, NY). 1981;212(4497):921–3.
38. Amar-Yuli I, Wachtel E, Shoshan EB, Danino D, Aserin A, Garti N. Hexosome and hexagonal phases mediated by hydration and polymeric stabilizer. Langmuir. 2007;23(7):3637–45.
39. Koegler WS, Patrick C, Cima MJ, Griffith LG. Carbon dioxide extraction of residual chloroform from biodegradable polymers. J Biomed Mater Res. 2002;63(5):567–76.
40. Mumper RJ, Jay M. Poly(L-lactic acid) microspheres containing neutron-activatable holmium-165: a study of the physical characteristics of microspheres before and after irradiation in a nuclear reactor. Pharm Res. 1992;9(1):149–54.
41. B'Hymer C. Residual solvent testing: a review of gas-chromatographic and alternative techniques. Pharm Res. 2003;20(3):337–44.
42. Freitas S, Merkle HP, Gander B. Microencapsulation by solvent extraction/evaporation: reviewing the state of the art of microsphere preparation process technology. J Control Release. 2005;102(2):313–32.
43. Zielhuis SW, Nijsen JF, Dorland L, Krijger GC, van Het Schip AD, Hennink WE. Removal of chloroform from biodegradable therapeutic microspheres by radiolysis. Int J Pharm. 2006;315 (1–2):67–74.